Stress-induced electric-dipole-allowed far-infrared generation at the spin-resonance frequency in InSb

C. Jagannath and R. L. Aggarwal*
Francis Bitter National Magnet Laboratory, Massachusetts Institute of Technology, Cambridge, Massachusetts 02139
(Received 16 August 1984; revised manuscript received 29 April 1985)

Using two CO_2 lasers operating at frequencies ω_1 ($=1075.98$ cm^{-1}) and ω_2 ($=973.30$ cm^{-1}), respectively, we have studied the stress-induced electric dipole spin-resonance contribution to the second-order nonlinearity $\chi^{(2)}$ in n-type InSb ($n_e \simeq 5\times10^{15}$ cm^{-3}) at 1.8 K via far-infrared (FIR) generation at $\omega_3=\omega_1-\omega_2$. With uniaxial stress X parallel to the magnetic field $\mathbf{B}||[111]$, propagation vectors $\mathbf{k}_1||\mathbf{k}_2||\mathbf{k}_3||[1\bar{1}0]$, and polarization vectors $\mathbf{E}_1||[11\bar{2}]$ and $\mathbf{E}_2||[111]$, we observe FIR radiation with $\mathbf{E}_3||\mathbf{B}$ at $X=0$. For $X\neq0$, we observe additional radiation with $\mathbf{E}_3\perp\mathbf{B}$, confirming the electric dipole contribution $\chi^{(2)}$. We have also observed a stress-induced decrease in the electron g factor, in agreement with calculated values.

I. INTRODUCTION

A number of experimental and theoretical studies have investigated far-infrared (FIR) generation by difference frequency mixing via spin-flip transitions in n-type InSb.[1–5] In the presence of a material excitation the second-order nonlinear susceptibility $\chi^{(2)}$, which characterizes the nonlinear interaction of the two pump beams at frequencies ω_1 and ω_2 to produce FIR output at $\omega_3=\omega_1-\omega_2$, exhibits resonance when ω_3 is equal to the frequency of the material excitation.[5] Further, $\chi^{(2)}$ is proportional to the matrix element of the interaction Hamiltonian connecting the initial and final states. Using the magnetic dipole interaction for the spin-flip FIR, Shen[5] calculated the resonance in $\chi^{(2)}$, in excellent agreement with results of Nguyen and Bridges.[2] Recently, it was shown by Trebin *et al.*[6] that uniaxial stress mixes the wave functions of the $n=1$ Landau level with those of the $n=0$ Landau level, thereby making the spin-flip transition "electric dipole allowed."[7] Since the matrix element for the electric dipole transition is typically orders of magnitude larger than that for the magnetic dipole transition, we would expect much larger $\chi^{(2)}$ for the electric dipole case.

In this paper we present results for the stress-induced electric-dipole-allowed FIR generation in n-type InSb. Experimental details are given in Sec. II. In Sec. III a brief outline of the theoretical background pertinent to our experimental arrangement, where the stress X is parallel to the magnetic field $\mathbf{B}||[111]$, is presented. The absorption coefficient α as well as $\chi^{(2)}$ is calculated. Taking into account the linewidth and the phase mismatch, the FIR output power P_{ω_3} is deduced. Comparison of the calculated and observed values for P_{ω_3}, discussed in Sec. IV, yields a value for the interband strain matrix element C_2. This value of C_2 is found to be smaller than those reported earlier.[7–9] Also, changes in the g factor with uniaxial stress are observed and theoretically explained.

II. EXPERIMENTAL

Two CO_2 transversely excited atmospheric (TEA) lasers operating at frequencies $\omega_1=1075.98$ cm^{-1} and $\omega_2=973.30$ cm^{-1} are used to generate FIR radiation at $\omega_3=\omega_1-\omega_2=102.68$ cm^{-1}. The input beams are cross polarized and propagate along a $[1\bar{1}0]$ crystal axis which is labeled x'. They are combined using a ZnSe beam splitter and focused on an InSb sample situated at the center of a superconducting magnet. The magnetic field $\mathbf{B}$ is parallel to a [111] crystallographic direction which is labeled z' axis. The electric vectors $\mathbf{E}_1$ and $\mathbf{E}_2$ of the input beams are parallel to $y'||[11\bar{2}]$ and z' axes so that $\mathbf{E}_1\perp\mathbf{B}$ and $\mathbf{E}_2||\mathbf{B}$. The sample with donor concentration $n_e=5\times10^{15}$ cm^{-3} is held between the stainless-steel cups at the bottom of a stress cell.[10] By pumping on the liquid helium surrounding the sample, the sample temperature is maintained at ~1.8 K. The uniaxial stress X is applied along the direction of the magnetic field. Typical sample dimensions were $3\times8\times15$ mm^3. The sample faces were polished using 0.25-μm diamond paste. Care was taken to polish the ends of the sample so as to achieve uniform stress; this allowed us to apply stresses up to ~4 kbar. Two quartz windows are used to filter out the CO_2 radiation and allow the FIR to pass through. A "pile of plates" polarizer,[11] consisting of 12 sheets each of 20- and 30-μm-thick polyethylene, is used to study the polarization $\mathbf{E}_3$ of the FIR output, using a Ge:In photoconductive detector.

III. THEORETICAL BACKGROUND

Theoretical aspects of the band structure of InSb in the presence of uniaxial stress have been analyzed by Trebin, Rössler, and Ranvaud.[6] Taking into account the Γ_6 conduction band and the spin-orbit-split Γ_8 and Γ_7 valence bands, the matrix Hamiltonian has the block form

$$\mathscr{H}=\begin{bmatrix} H_{cc} & H_{cv} & H_{cs} \\ H_{vc} & H_{vv} & H_{vs} \\ H_{sc} & H_{sv} & H_{ss} \end{bmatrix},$$

where H_{cc}, H_{vv}, and H_{ss} are 2×2, 4×4, and 2×2 matrices describing the Γ_6, Γ_8, and Γ_7 bands. H_{cv} and H_{cs} represent the interactions of the Γ_6 conduction band with the Γ_8 and Γ_7 valence bands. H_{vs} is the interaction between Γ_8 and Γ_7 bands. These matrices are explicitly given in Table IV of Ref. 6. In a first approximation H_{sv} is neglected and the Schrödinger equation for the conduction-band envelope functions reduces to a matrix equation

$$(-E+H_0+H_X)\begin{bmatrix} f_1 \\ f_2 \end{bmatrix}=0\ , \tag{1}$$

where

$$H_0=\frac{P^2}{3}\left[\left[\frac{2}{E_g+E}+\frac{1}{E_g+\Delta+E}\right]k^2 - \left[\frac{1}{E_g+E}-\frac{1}{E_g+\Delta+E}\right]\frac{e}{\hbar}\mathbf{B}\cdot\boldsymbol{\sigma}\right] \tag{2}$$

is the strain-independent part and

$$H_X=\tfrac{2}{3}PC_2\left[\frac{1}{E_g+E}-\frac{1}{E_g+\Delta+E}\right] \times[\sigma_x(\epsilon_{zx}k_z-\epsilon_{xy}k_y)+\text{c.p.}] \tag{3}$$

is that part of the strain-dependent perturbation which causes wave-function mixing. Here P and C_2 are the interband matrix elements for momentum and strain operators, respectively, $\mathbf{k}$ is the momentum operator, E_g is the band gap, Δ is the spin-orbit splitting of the valence band, σ is the Pauli spin matrix, ϵ_{zx}, ϵ_{xy}, etc. are components of the strain tensor, and c.p. denotes cyclic permutations. H_X causes mixing of the wave functions of the Landau subbands. Using first-order perturbation theory, the envelope wave functions of the Landau levels can be determined. In particular, for $\mathbf{B}||X||[111]$, Eq. (3) reduces to

$$H_X=\begin{bmatrix} 0 & -idk_- \\ idk_+ & 0 \end{bmatrix}\ , \tag{4}$$

where

$$d=\tfrac{2}{3}PC_2\left[\frac{1}{E_g+E}-\frac{1}{E_g+\Delta+E}\right]S_{44}\frac{\sqrt{6}}{6}X \tag{5}$$

and $k_\pm=(1/\sqrt{2})(k_{x'}\pm ik_{y'})$. The envelope wave functions of the $n=0$ Landau levels are

$$f_1=\phi_0^\uparrow-\frac{id}{l}\left[\frac{\phi_1^\downarrow}{E_1^\downarrow-E_0^\uparrow}\right]\ , \tag{6a}$$

$$f_2=\phi_0^\downarrow\ , \tag{6b}$$

where $\uparrow$ and $\downarrow$ represent spin up and spin down, respectively, ϕ_0 and ϕ_1 are the unperturbed (i.e., zero stress) envelope wave functions for the $n=0$ and $n=1$ Landau levels, and $l=\sqrt{\hbar/eB}$ is the magnetic length. From Eqs. (6a) and (6b) it follows that

$$\langle f_2\,|\,k_+\,|\,f_1\rangle=0\ , \tag{7a}$$

$$\langle f_2\,|\,k_-\,|\,f_1\rangle=c_1/l\ , \tag{7b}$$

$$\langle f_2\,|\,k_z\,|\,f_1\rangle=0\ , \tag{7c}$$

with

$$c_1=-\frac{id}{l}\left[\frac{1}{E_1^\downarrow-E_0^\uparrow}\right]\ . \tag{7d}$$

In order to calculate the absorption coefficient associated with the magnetic dipole ($X=0$) and the stress-induced electric dipole transitions we start with the equation

$$\alpha(\omega)=\frac{n_e}{2N(\omega)\hbar^2}\frac{\Gamma}{(\omega-\omega_s)^2+\Gamma^2}\,|\,\langle f_2\,|\,H'\,|\,f_1\rangle\,|^2\ , \tag{8}$$

where $N(\omega)$ is the photon flux at frequency ω, Γ is the half-width at half-maxima for the absorption line, and H' is the amplitude of perturbation due to the electromagnetic radiation. For the electric dipole case

$$H'_{\mathrm{ED}}=\frac{e}{m^*}\mathbf{A}_\omega\cdot\mathbf{p}\ , \tag{9}$$

where $\mathbf{A}_\omega$ is the vector potential of the radiation field. For the magnetic dipole transition, the corresponding perturbation is

$$H'_{\mathrm{MD}}=\tfrac{1}{2}g^*\mu_B\boldsymbol{\sigma}\cdot\mathbf{B}_\omega\ , \tag{10}$$

$\mathbf{B}_\omega$ being the magnetic field associated with the radiation field. Using Eqs. (8) and (9) the absorption coefficient associated with the electric dipole spin resonance is

$$\alpha_{\mathrm{ED}}(\omega)=\left[\frac{e^2}{4\pi\epsilon_0\hbar c}\right]\frac{4\pi n_e}{\eta(m^*)^2\omega} \times|\,\langle f_2\,|\,\mathbf{p}\cdot\hat{\mathbf{e}}\,|\,f_1\rangle\,|^2\frac{\Gamma_{\mathrm{ED}}}{(\omega-\omega_s)^2+\Gamma_{\mathrm{ED}}^2}\ , \tag{11}$$

where $\hat{\mathbf{e}}$ is a unit vector along the electric field $\mathbf{E}_\omega$ of the radiation, m^* is the effective mass of the conduction electron, and $n\rightarrow\eta$ is the refractive index. Assuming $\hat{\mathbf{e}}$ is along the x' axis,

$$\mathbf{p}\cdot\hat{\mathbf{e}}=\frac{\hbar}{\sqrt{2}}(k_++k_-)\ . \tag{12}$$

Substituting Eq. (12) into Eq. (11) and using Eqs. (7a) and (7b), we get

$$\alpha_{\mathrm{ED}}(\omega)=\left[\frac{e^2}{4\pi\epsilon_0\hbar c}\right]\frac{4\pi n_e m_s^*}{\eta(m^*)^2\omega} \times\frac{\Gamma_{\mathrm{ED}}}{(\omega-\omega_s)^2+\Gamma_{\mathrm{ED}}^2}\left[\frac{\hbar\omega_s}{2}\right]|\,c_1\,|^2\ , \tag{13}$$

where c_1 is given by Eq. (7d) and $m_s^*=|\,2m/g^*\,|$ is the effective spin mass. Similarly, one can show that the absorption coefficient for magnetic dipole spin resonance for the polarization $\hat{\mathbf{e}}$ along the z' axis is given by

$$\alpha_{\mathrm{MD}}(\omega)=\left[\frac{e^2}{4\pi\epsilon_0\hbar c}\right]\frac{\pi n_e\hbar^2\omega\eta}{(m_s^*)^2c^2}\frac{\Gamma_{\mathrm{MD}}}{(\omega-\omega_s)^2+\Gamma_{\mathrm{MD}}^2}\ . \tag{14}$$

The ratio of the peak values of α_{ED} and α_{MD} is obtained from Eqs. (13) and (14) as

$$\frac{\alpha_{ED}(\omega_s)}{\alpha_{MD}(\omega_s)}=\frac{2}{\eta^2}\left[\frac{m_s^*}{m^*}\right]^2\frac{m_s^* c^2}{\hbar\omega_s}\left[\frac{\Gamma_{MD}}{\Gamma_{ED}}\right]|c_1|^2 . \quad (15)$$

Following the analysis outlined by Shen,[5] we can calculate the $\chi^{(2)}$ due to the electric and magnetic dipole spin-resonance transitions. Assuming that the input fields E_1 and E_2 are along the y' and z' directions, respectively, with the input and output beams propagating along the x' direction, we obtain

$$\frac{|\chi^{(2)}_{ED}|^2}{|\chi^{(2)}_{MD}|^2}=\frac{\alpha_{ED}(\omega_s)}{\alpha_{MD}(\omega_s)} . \quad (16)$$

Thus it would be useful to estimate a value for $\alpha_{ED}(\omega_s)/\alpha_{MD}(\omega_s)$, using the known values of the parameters appropriate for InSb. With $P=9.0\times10^{-8}$ eV cm (Ref. 12), $E_g=0.235$ eV, $\Delta=0.803$ eV (Ref. 13), and $S_{44}=3.18\times10^{-3}$/kbar (Ref. 14), Eq. (5) gives $d/X=2.56\times10^{-12}\ C_2$. Taking $B=53$ kG, $E_1^{\downarrow}-E_0^{\uparrow}\simeq0.047$ eV, Eq. (7d) then yields $|c_1|/X=4.9\times10^{-3}\ C_2$/kbar. Using this value of $|c_1|/X$ along with $|g^*|=41.8$ and $m^*=0.015m$, Eq. (15) gives

$$\frac{\alpha_{ED}(\omega_s)}{\alpha_{MD}(\omega_s,X=0)}=5.65\times10^2(C_2X)^2\frac{\Gamma_{MD}(X=0)}{\Gamma_{ED}} . \quad (17)$$

Considering both the phase mismatch and absorption, the FIR power is given by[15]

$$P_{\omega_3}\propto|\chi^{(2)}|^2L^2e^{-\alpha_3L}\frac{1+e^{-\Delta\alpha L}-2e^{-\Delta\alpha L/2}\cos(\Delta kL)}{(\Delta kL)^2+(\Delta\alpha L/2)^2} , \quad (18)$$

where L is the length of the crystal along the direction of propagation, and

$$\Delta k=k_1-k_2-k_3 , \quad (19a)$$

$$\Delta\alpha=\alpha_1-\alpha_2-\alpha_3 . \quad (19b)$$

Here the subscripts 1, 2, and 3 refer to the frequencies ω_1, ω_2, and ω_3, respectively. When $\alpha_1=\alpha_2\simeq0$ (as is the case in our experiment), $\Delta\alpha=-\alpha_3=-(\alpha^{FC}+\alpha')$, where α^{FC} is the free-carrier absorption and α' is either α_{ED} or α_{MD} as the case may be. In order to calculate Δk and α^{FC} we consider both the phonon and free-carrier contributions to the refractive index.[16] Assuming that $\alpha^{FC}=20$ cm^{-1} for $\mathbf{E}_3||\mathbf{B}$ we find that for $B=53$ kG, $\Delta k_{MD}=-7.5$ cm^{-1}, and $\alpha^{FC}=20$ cm^{-1} for the magnetic-dipole-allowed FIR, whereas $\Delta k_{ED}=-43.4$ cm^{-1} and $\alpha^{FC}=3.0$ cm^{-1} for the stress-induced electric-dipole-allowed FIR. Using these values of Δk and α^{FC} along with $L=0.3$ cm and $\alpha_{MD}=0.188$ cm^{-1} at $X=0$ (as discussed in Sec. IV), the ratio $P^{ED}_{\omega_3}(X)/P^{MD}_{\omega_3}(0)$ can be easily calculated.

IV. RESULTS AND DISCUSSION

Figure 1 shows the FIR output P_{ω_3} as a function of B. For $X=0$ and $\mathbf{E}_3||\mathbf{B}$, a sharp resonance in P_{ω_3} is observed at $B=52.57$ kG. No such resonance is seen for $\mathbf{E}_3\perp\mathbf{B}$, as expected for the magnetic-dipole-allowed transitions. The half-width at half-maxima of this line is 0.085 kG, in good agreement with that observed in the transmission experiments.[17] It it interesting to note that the line exhibits pronounced asymmetry, clearly evident in the inset of Fig. 1. Such asymmetry is in qualitative agreement with the theoretical predictions of Yuen *et al.*[18] in terms of the collision-broadened density of states in a magnetic field. The FIR output for $\mathbf{E}_3\perp\mathbf{B}$ is shown in Fig. 1 for $X=1.12$, 1.67, and 2.24 kbar. For the $X\neq0$ data, we note (i) the peak of the resonance shifts to higher B with increasing X, indicating a decrease in the g factor, (ii) the linewidth (half-width at half-maxima) of the peak is ~0.9 kG for $0.5\leq X\leq2.24$ kbar (this may arise from the decrease in the spin-relaxation time due to the stress-induced mixing of the wave functions), and (iii) a new feature, indicative of a second resonance, is observed; the two resonance peaks probably correspond to the free and the impurity-bound electrons.[7,17]

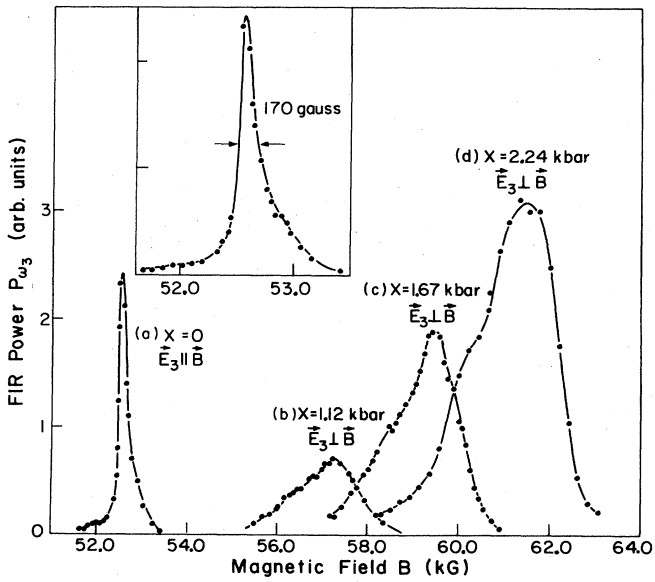

FIG. 1. Far-infrared power P_{ω_3} as a function of magnetic field $\mathbf{B}||[111]$ for n-type InSb ($n_e=5\times10^{15}$ cm^{-3}) at 1.8 K with uniaxial stress $X||[111]$. (a) $X=0$, FIR polarization $\mathbf{E}_3||\mathbf{B}$; (b) $X=1.12$ kbar, $\mathbf{E}_3\perp\mathbf{B}$; (c) $X=1.67$ kbar, $\mathbf{E}_3\perp\mathbf{B}$; (d) $X=2.24$ kbar, $\mathbf{E}_3\perp\mathbf{B}$.

We wish to point out that for the geometry of this experiment, i.e., $\mathbf{B}||[111]$, the inversion-asymmetry-induced electric dipole spin-resonance transition is not allowed in the longitudinal Voigt ($\mathbf{E}||\mathbf{B}$, i.e., π polarization) geometry.[19] Thus for $\mathbf{E}_3||\mathbf{B}$ we attribute the observed FIR radiation at $\omega_3=\omega_s$ to the magnetic-dipole-allowed spin resonance. No FIR radiation was observed for $\mathbf{E}_3\perp\mathbf{B}$ at $X=0$; this implies that the contribution of asymmetry-induced electric dipole spin resonance is negligible for the sample geometry used in this experiment.[20]

Using the observed value $\Gamma_{MD}(X=0)=0.085$ kG, $m_s^*=2m/g^*=0.048m$, $n_e=5\times10^{15}$ cm^{-3}, $\eta=4.08$, and $\hbar\omega_s=102.68$ cm^{-1}. Equation (14) gives $\alpha_{MD}(\omega_s,X=0)=0.188$ cm^{-1}. With these values of $\Gamma_{MD}(X=0)$, $\alpha_{MD}(\omega_s,X=0)$, and $\Gamma_{ED}=0.9$ kG, Eq. (17) yields $\alpha_{ED}(\omega_s)=1.00(C_2X)^2$ cm^{-1}. For these values of

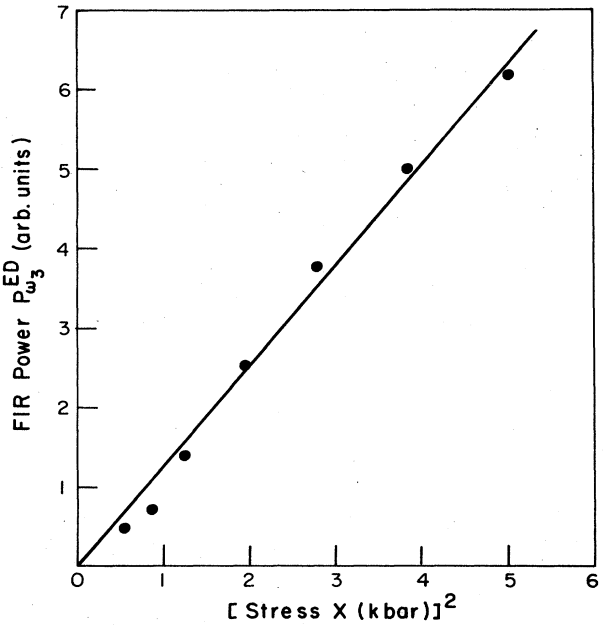

FIG. 2. Far-infrared power as a function of X^2. The solid line is the least-squares fit to the data shown by dots.

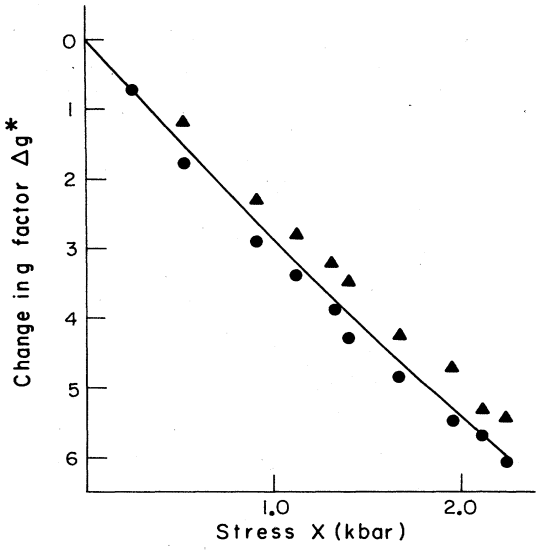

FIG. 3. Change in the electron g factor Δg^* as a function of stress. The solid circles and triangles are experimental data. The solid line is the calculated curve.

$\alpha_{\rm MD}(\omega_s, X=0)$ and $\alpha_{\rm ED}(\omega_s)$, and the observed value of $P_{\omega_3}^{\rm ED}(2.24\ \text{kbar})/P_{\omega_3}^{\rm MD}(0)=1.3$, we obtain $|C_2|=1.0$ eV. This is smaller than the value of 1.6 ± 0.5 eV obtained by measuring the absorption coefficient[7] for the stress-induced electric dipole spin-flip resonance.

The important source of error in our measurement of $|C_2|$ are as follows: (i) The error in the observed value of $P_{\omega_3}^{\rm ED}/P_{\omega_3}^{\rm MD}$ is estimated to be $\pm20\%$, which corresponds to a $\pm10\%$ error in the value of $|C_2|$. (ii) It is known[19,20] that in the longitudinal Voigt configuration, $\mathbf{E}||\mathbf{B}||[111]$, the inversion-asymmetry-induced electric dipole spin resonance is not allowed. However, misorientation of $\sim1°$ could result in an absorption coefficient of $\sim0.02\ \text{cm}^{-1}$, which is $\sim10\%$ of $\alpha_{\rm MD}$. The misorientation results in a lowering of the observed value of $|C_2|$. (iii) The uncertainty in the calculated values of $\Delta k_{\rm MD}$ and $\Delta k_{\rm ED}$. We estimate the overall error of $\pm30\%$, so that $|C_2|=1.0\pm0.3$ eV.

Figure 2 shows the peak value of the electric dipole FIR power output as a function of X^2. The observed X^2 dependence of FIR power output is consistent with our calculations.

Figure 3 shows the stress-induced decrease in the g factor. The solid circles and triangles represent the experimental data for the peaks at higher and lower magnetic fields, respectively. It should be pointed out that for the geometry used in Ref. 7, $X||[110]$ with $\mathbf{B}||[1\bar{1}2]$, the stress dependence of the g factor was found to be small, both experimentally and theoretically.[7] The observed stress-induced decrease in the g factor for our geometry $X||\mathbf{B}||[111]$ can be calculated by considering the shifts in the conduction- and valence-band edges. For $X||[111]$, the energy shift for the conduction band is given by

$$\Delta E_c = D_d^c(S_{11}+2S_{12})X\ , \tag{20}$$

where D_d^c is the hydrostatic deformation-potential constant of the conduction band; S_{11} and S_{12} are the compliance constants. The corresponding shift for the valence band is

$$\Delta E_v = [D_d^v(S_{11}+2S_{12}) \pm \tfrac{1}{3}D_u' S_{44}]X\ , \tag{21}$$

where D_d^v and D_u' are the hydrostatic and shear deformation-potential constants for the valence band, respectively. The second term in Eq. (21) represents one-half of the stress-induced splitting of the $M_J=\pm\frac{3}{2}$ and $\pm\frac{1}{2}$ states. By including these terms along the diagonal in the H_{cc} and H_{vv} matrices of Eq. (1), we have calculated g^* as a function of stress, using the Pidgeon and Brown model.[21] The solid line in Fig. 3 represents these calculations, using[9,14] $D_d^c - D_d^v = -7.0$ eV, $D_u' = 4.10$ eV, $S_{11}=2.261\times10^3$/kbar, $S_{12}=-0.764\times10^{-3}$/kbar, and $S_{44}=3.180\times10^{-3}$/kbar. The results in Fig. 3 are in good agreement between calculated and observed values of the stress-induced changes in g^*.

ACKNOWLEDGMENTS

We wish to thank Professor P. A. Wolff for bringing this problem to our attention and for his encouragement during the course of this work. We thank Dr. F. Kuchar and Dr. M. Kriechbaum for stimulating discussions. This work was supported by the Air Force Office of Scientific Research Contract No. F49620-84-C-0010. The Francis Bitter National Magnet Laboratory is supported by the National Science Foundation through its Division of Materials Research under Contract No. DMR-8211416.

*Also at Department of Physics, MIT.
[1]N. V. Tran and C. K. N. Patel, Phys. Rev. Lett. **22**, 463 (1969).
[2]V. T. Nguyen and T. J. Bridges, Phys. Rev. Lett. **29**, 359 (1972).
[3]T. L. Brown and P. A. Wolff, Phys. Rev. Lett. **29**, 362 (1972).
[4]E. D. Shaw, Appl. Phys. Lett. **29**, 28 (1976).
[5]Y. R. Shen, Appl. Phys. Lett. **23**, 516 (1973).
[6]H.-R. Trebin, U. Rössler, and R. Ranvaud, Phys. Rev. B **20**, 686 (1979).
[7]M. Kriechbaum, R. Meisels, F. Kuchar, and E. Fantner, in *Proceedings of the 16th International Conference on the Physics of Semiconductors, Montpellier, France, 1982,* edited by M. Averous (North-Holland, Amsterdam, 1983), p. 444.
[8]D. G. Seiler, B. D. Bajaj, and A. E. Stephens, Phys. Rev. B **16**, 2822 (1977).
[9]R. Ranvaud, H.-R. Trebin, U. Rössler, and F. H. Pollak, Phys. Rev. B **20**, 701 (1979).
[10]The stress cell used in the present experiment is similar in principle to the one described by Tekippe *et al.*, Phys. Rev. B **6**, 2348 (1972). Modifications were made in the design so as to immerse it in the liquid helium present in the sample chamber of the superconducting magnet.
[11]A. Mitsuishi, Y. Yamada, S. Fujita, and H. Yoshinaga, J. Opt. Soc. Am. **50**, 433 (1960).
[12]C. R. Pidgeon and S. H. Groves, Phys. Rev. **186**, 824 (1969).
[13]R. L. Aggarwal, in *Semiconductors and Semimetals,* edited by R. K. Willardson and A. C. Beer (Academic, New York, 1972), Vol. 9, p. 151.
[14]R. F. Potter, Phys. Rev. **102**, 47 (1956).
[15]See, for example, R. L. Aggarwal, in *Topics in Applied Physics,* edited by Y. R. Shen (Springer-Verlag, Berlin, 1977), Vol. 16, p. 19.
[16]See, for example, E. D. Palik, and G. B. Wright, in *Semiconductors and Semimetals,* edited by R. K. Willardson and A. C. Beer (Academic, New York, 1967), Vol. 3, p. 421.
[17]B. D. McCombe, in Proceedings of the International Conference on the Application of High Magnetic Fields in Semiconductor Physics, Würzburg, Federal Republic of Germany, 1974 (unpublished), p. 146.
[18]S. Y. Yuen, P. A. Wolff, and B. Lax, Phys. Rev. B **9**, 3394 (1974).
[19]M. H. Weiler, R. L. Aggarwal, and B. Lax, Phys. Rev. B **17**, 3269 (1978).
[20]M. Dobrowolska, Y. Chen, J. K. Furdyna, and S. Rodriguez, Phys. Rev. Lett. **51**, 134 (1983).
[21]C. R. Pidgeon and R. N. Brown, Phys. Rev. **146**, 575 (1966).